Femtosecond Optical Spectroscopy of High T_c Superconductors and Fullerites

V. M. Farztdinov, Yu. E. Lozovik, Yu. A. Matveets
Institute of Spectroscopy, Russian Academy of Sciences
142092 Troitsk, Moscow Region, Russia
E-mail: Lozovik@isan.msk.su

Received March 20, 1995

Femtosecond laser spectroscopy is used to study the temporal behavior of the optical spectra of the films of $YBa_2Cu_3O_{7-\delta}$ and C_{60} on a 100-fs scale. The studies cover initial ternperature dependence of the optical spectra of superconductors and laser intensity dependence of the fullerites absorption. The appearance of the superconducting energy gap in the optical spectra (in the region of photon energies that are substantially higher than the superconducting energy gap) is investigated. It is shown both experimentally and theoretically that in the difference spectrum of the $\epsilon_2(\omega)$ between the superconducting and normal phases there is a characteristic structure which width is connected with the energy gap. Based on the experimental data, the electron-phonon interaction parameter $\lambda < \omega^2 >$ has been estimated at 450 ± 150 (meV)^2. The rise of absorption in fullerites, peaked at zero delay times, is shown to be replaced by electronic-vibrational relaxation with times $\tau_1 \approx 1$ ps and $\tau_2 \approx 1$ ps. Relaxation mechanisms corresponding to these times are discussed. Simple theory of the fullerite photodarkening dependence on the energy density of the femtosecond laser pulse is presented. The physical effects that appear at high excitation levels are discussed.

I. Introduction

Femtosecond laser spectroscopy enables one to study in real time various processes taking place in solids and to observe changes of electronic spectra in the course of the formation of new phases, and so on (see, for example, Refs. 1 and 2 and references cited therein). For example, real-time studies into the relaxation of charge carriers in oxide superconductors and doped fullerites (M_xC_{60}) offers a unique possibility to directly determine electron-phonon interaction constants and to observe the formation or destruction kinetics of the superconducting order parameter. As a result one can obtain a unique information about the nature of superconductivity in such materials, particularly the role of electron-phonon interaction in them.

Magnitude and symmetry of the superconducting order parameter in oxide based materials and fullerides continue to be a topic of active study. Apart from traditional techniques (such as infrared, tunneling and Raman spectroscopy; see, e.g. Ref [3]), femtosecond laser spectroscopy[4-6] is promising for energy gap determination.

Another reason for studying the femtosecond dynamics of optical spectra of C_{60} is that it may be a useful material because of its nonlinear optical properties; accordingly, the ultimate speed of its nonlinear optical response is of great practical interest.

In this review we would describe some of our investigations of the femtosecond dynamics of the difference optical spectra of an and C_{60} films with the help of the femtosecond laser spectroscopy.

The aims of this studies were the following:

- study of the femtosecond charge carrier dynamics in HTSC $YBa_2Cu_{30}O_{7-\delta}$;

- estimation of the electron-phonon interaction parameter $\lambda < \omega^2 >$ and electron-phonon coupling constant λ;

- investigation of the appearance of the superconducting energy gap in the optical spectra (in the region of interband transitions with $\hbar\omega >> \Delta$);

- study of nonlinear optical properties of solid C_{60} on the femtosecond time scale;

- investigation of the photodarkening dependence on the energy of the femtosecond laser pulse.

II. The essentials of femtosecond spectroscopy

Femtosecond optical spectroscopy, along with other modulation spectroscopy methods is an important method for studying the critical points in band structure associated with interband optical absorption in solids. It has some advantages over others for it also enables scientists to investigate the dynamics of nonequilibrium charge carrier's relaxation, and to set apart the changes of optical properties caused by nonequilibrium distribution of charge carriers and phonons. Femtosecond optical spectroscopy of metals makes it feasible to select for a narrow spectral region transitions from some valence band to the states near the Fermi level (FL)[7−12] and to observe the dynamics of carriers and lattice temperatures.

Really an increase of the electron temperature due to the action of a pump pulse leads to the following processes:

(1) Fermi level smearing that results in the opening of states below the FL and to the population of the states above the FL. This affects all interband transitions that originate or terminate on states near the Fermi level and leads to an increase of the contributions into the dielectric function $\epsilon_2(\omega)$ of the interband transitions to the states below FL and to decrease of the contributions into $\epsilon_2(\omega)$ of the interband transitions to the states above FL.

(2) Shift of the FL. In good metals this is small effect, but in poor metals it can be significant.

An increase of the lattice temperature due to transfer of energy from electrons to phonons leads to the following processes:

(4) Volume thermal expansion causes shifts and warping in the electron energy bands through changes in the one-electron potential. Changes in the bands cause the FL to shift. Thermal expansion also decreases the plasma frequency.

(5) If the sample is constrained by the substrate, thermal expansion also causes shear strains. These can split degenerate energy bands and cause shifting and warping as well. The latter could affect the FL.

All of these effects contribute to $\Delta\epsilon_2(\omega)$ at a particular photon energy, if the band structure permits. At time delays shorter than electron-phonon relaxation time only the contributions of the first two effects are dominant. As a result of these effects the change of $\epsilon_2(\omega)$ appears as a characteristic structure with sign reversal at ω_F, corresponding to the transitions to (or from) the FL. Thus, the spectral position of the FL can be found from the condition $\Delta\epsilon_2(\omega_F) = 0$[7 − 12].

Once the transitions into the FL region for some pare of bands are selected, then one can observe a feature in the difference optical spectrum between the superconducting and normal phases and its width as will be shown below is connected with the superconducting energy gap.

III. Experimental technique[8,63]

The experimental setup was a standard configuration and consisted of a master generator, an amplifier, and a measuring block. The master generator (a ring-type colliding-pulse laser) generated a continuous train of pulses 90 fs in duration and 100 MHz in repetition frequency at a wavelength of 615 nm ($\hbar\omega$ = 2.02 eV). The output from the generator was fed to the input of the 4-stage dye- laser amphfier. The amplifier was pumped by an excimer laser with 3 Hz in pulse frequency, which determined the pulse repetition rate at the output of the laser system. The pulses from the amplifier output were fed to the measuring block of the experimental setup. The duration of the amplified laser pulses amounted to 100 fs in the experiments on fullerites and to 150 fs in the experiments on the superconductors.

In the measuring block, laser radiation was divided into two channels - the exciting channel and the probing channel. In the exciting channel, the laser pulses were focused onto the sample to be studied. The exciting beam spot on the sample was 100 μm across. The excitation density could be varied from approximately 10^{10} to to 10^{13} W/cm^2 by means of neutral optical filters and also by changing the beam focusing. In the probing channel, the laser pulses were first focused into a cell filled with heavy water in order to convert them into broadband pulses of the same duration. These pulses were then focused on the sample inside the excitation spot. The probing beam spot was 50 μm across. The probing pulses that passed through (or reflected from) the sample were detected by an optical multichannel analyzer built around two charge-coupled-device (CCD) arrays. Probing was effected in different ranges around of 2 eV. For example in studies of fullerites it was in the range 1.8-2.3 eV. Temporal resolution was attained by varying the optical delay between the exciting and probing pulses. The minimum delay variation step came to 35 fs. The maximum delay

time reached 10 ps. The repetition frequency of the exciting and probing pulses amounted to approximately 1 Hz. Measurements of fullerites were taken at room temperature in air. Throughout the experiment, we have controlled the optical density of the sample and have not found any irreversible changes in it.

The samples under study

The sample under study was a 150 nm thick $YBa_2Cu_{30}O_{7-\delta}$ film deposited on a $SrTiO_3$ substrate and coated with a protective MgO layer 5 nm in thickness. The superconducting and protective layers were grown by high-frequency magnetron sputtering in a single production cycle. The crystallites in the superconducting layer were around 300 nm across, their c-axis being oriented normal to the substrate surface. The critical temperature T_c was equal to 80 K.

Another sample under study – a C_{60} film with a thikness of approximately 1 μm on a quartz substrate - was excited with optical pulses with a duration of some 100 fs and a photon energy of $\hbar\omega_p = 2.02$ eV much in excess of the band gap $E_g \sim 1.7$ eV. Measurements were taken at room temperature in air. Throughout the experiment, we have controlled the optical density of the sample and have not found any irreversible changes in it.

IV. Superconductors. Theory and experiment

IV.1. Superconducting energy gap in the optical spectra. Theory [13-15].

The nature of the superconducting state and the superconducting order parameter in high T_c superconductors are still matters of controversy. Theoretical model studies (see [16-17]) have indicated that the superconducting gap of high T_c superconductors might have a d-wave symmetry, contrary to the s-wave symmetry in ordinary superconductors. Although some experiments can be interpreted in the framework of one or other d-wave superconductor model[18−20], a lot of experimental results[21−22] are consistent with s-wave symmetry of the superconducting order parameter. Here we shall consider mostly the s-wave pairing.

Traditional viewpoint on the optical properties of superconductors is that in the optical spectra with the photon energies $\hbar\omega \gg \Delta$ one cannot see any differencies between superconducting and normal states. And this viewpoint is quite write until you don't investigate the frequency range, corresponding to the interband transitions to the states near the Fermi level. Here we shall consider such transitions in detail.

Suppose that for some superconducting metal a narrow spectral region corresponding to the transitions from some valence band (v) to the states near the Fermi level in the conductivity band (c) was determined. (The consideration of the transitions from the states near the Fermi level to an upper conductivity band is quite similar.) Then for this narrow spectral region the dielectric function can be written as $\epsilon(\omega) = \epsilon_0 + \epsilon^{cv}(\omega)$, where $\epsilon^{cv}(\omega)$ accounts for a contribution of the given pair of bands and ϵ_0 accounts for the nonresonant contribution of all other transitions. The expression for the linear response of superconductor in the *interband* transition region differs from the known expressions[23] for intraband transitions at frequencies. For the imaginary part of the dielectric function $\epsilon_2^{cv}(\omega)$ one can obtain the following relation

$$\begin{aligned}\epsilon_2^{cv}(\omega) &= \frac{A}{\omega^2}\int_0^\infty dx\{[\tanh\epsilon/2T + \tanh\eta/2T]u^2\delta(\epsilon+\eta-\omega) \\ &- [\tanh\epsilon/2T - \tanh\eta/2T]\nu^2\delta(\epsilon-\eta+\omega)\} \qquad (1)\end{aligned}$$

where $x = |p^2/2m_c|$; $\epsilon = \sqrt{(x-\mu)^2+\Delta^2}$; $\eta = x|g|\mathrm{sign}(m_c) + \mu + E_g$; $g = -m_c/m_v$; $u^2 = [1 + \mathrm{sign}(m_c)(x-\mu)/\epsilon]/2$; $\nu^2 = [1 - \mathrm{sign}(m_c)(x-\mu)/\epsilon]/2$; $A = 4e^2|P|^2|m_c|/m^2\Omega^2$. Here P is the matrix element of the momentum between corresponding Bloch states (as we are interested in a narrow region near FL we suppose that P is independent of the momentum p); m_c and m_v are the effective masses in the c- and v-band,

respectively; μ is the FL; E_g is the $c-v$ band gap, Δ is the superconducting gap; m is the mass offree electron; Ω is the elementary cell volume.

To represent the layered structure common to copper oxides we assumed the dispersion laws of valence and conduction bands to be two dimensional and isotropic. We also supposed that they have the extremum in the same point of a Brillouin zone. The integrals in Eq. (2) can be readily calculated and we get

$$\begin{aligned}\epsilon_{2cv}(\omega) &= \frac{A}{2\omega^2|1+g|}\left[\left(\mathrm{sign}(m_c)+\frac{\tilde{\omega}}{\sqrt{\tilde{\omega}^2-\tilde{\Delta}^2}}\right)\left(1+\tanh\frac{\tilde{\omega}-|g|\sqrt{\tilde{\omega}^2-\tilde{\Delta}^2}}{2T(1-g^2)}\right)\times\right.\\ &\times\ [\Theta(1-|g|)[\Theta(\tilde{\omega}-\tilde{\Delta})-[\Theta(-\tilde{\omega}-\tilde{\Delta})]+\mathrm{sign}(m_c)\Theta(|g|-1)\Theta(\tilde{\omega}-\omega_1)]-\\ &-\ \left(\mathrm{sign}(m_c)-\frac{\tilde{\omega}}{\sqrt{\tilde{\omega}^2-\tilde{\Delta}^2}}\right)\left(1+\tanh\frac{\tilde{\omega}+|g|\sqrt{\tilde{\omega}^2-\tilde{\Delta}^2}}{2T(1-g^2)}\right)\times\\ &\times\ \left.[\Theta(1-|g|)[\Theta(\omega_1-\tilde{\omega})\Theta(\tilde{\omega}-\tilde{\Delta})-\Theta(\tilde{\omega}-\omega_2)\Theta(-\tilde{\omega}-\tilde{\Delta})]]-\mathrm{sign}(m_c)\Theta(|g|-1)\Theta(\tilde{\omega}-\omega_2)\right] \quad (2)\end{aligned}$$

where $\tilde{\omega}=\omega-E_g-\mu\mathrm{sign}(m_c)(1+g)$, $\tilde{\Delta}^2=\Delta^2(1-g^2)$, $\tilde{\Delta}=\Delta\sqrt{|1-g^2|}$, $\omega_{1,2}=\pm\sqrt{\mu^2+\Delta^2}-\mu|g|$, $\Theta(\omega)$ is theta- function (we suggest here that the temperature does not change the valence band occupation).

The relaxation processes, mainly due to electron-phonon interaction, for electrons near the Fermi surface can be taken into account phenomenologically using the convolution of $\epsilon_2^{cv}(\omega)$ with the factor $\exp(-\omega^2/\gamma 2)/\sqrt{\pi\gamma}$, the parameter γ connected with the relaxation rate (it corresponds to the substitution $i0\rightarrow i\gamma$ in eq.(3)):

$$\epsilon_2^{cv}(\omega,\gamma,T)=\int d\omega'\exp(-\omega'^2/\gamma^2)\epsilon_2^{cv}(\omega+\omega',\gamma,T)/\sqrt{\pi\gamma}\,.$$

For illustration, we present our results on Figs.(1-3) for $1/\gamma\approx 500$ fs, this value corresponding to $YBa_2Cu_{30}O_{7-\delta}$ (see Refs. [8,10]).

To study of the optical properties of the superconductors with high T_c, the transitions between various bands with the arbitrary effective masses (including masses with opposite signs) can be used. The femtosecond spectroscopy makes it feasible to select for a narrow spectral region the transitions from some valence band to the states near the FL. Therefore, it is of interest to analyze the expression for $\Delta\epsilon_2(\omega)$ for different dispersion laws in c- and v-bands (i.e., for different signs and relative values of effective masses m_c and m_v, see insets in Figs(1-3)).

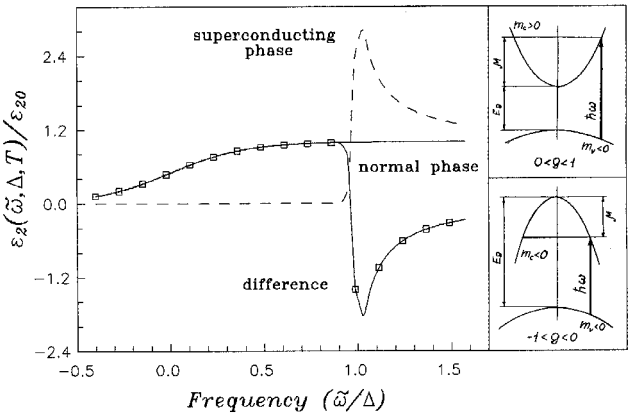

Figure 1. The imaginary part of the dielectric function, corresponding to the interband transitions in the case $g=0.2$; $\epsilon_{20}=\epsilon_2(\tilde{\omega}=0,\Delta=0,T=0)$. The dashed, solid and solid with squares lines correspond the superconducting phase (for $\Delta=30$ meV, $T=63$ K), to the norrnal phase (for $T=92$ K) and to the difference between them in the case $\mu/\Delta\gg 1$, respectively. Insets: Diagram of interband transitions from the heavy effective mass band to the light effective mass band $|g|<1$.

Consider the possible manifestations of interband transitions for $YBa_2Cu_{30}O_{7-\delta}$ superconductors. FL in $YBa_2Cu_{30}O_{7-\delta}$ crosses a number of bands with different effective masses (see [24-31]). In the vicinity of the S point of two-dimensional Brillouin zone (BZ) (or the line SR of three dimensional BZ) the following optical transitions can occur.

(1) Transitions from the lower bands of heavy carriers with $m_v < 0$ (formed by Cu2(3d)O2(p)-O3(p) orbitals) to the states of conduction band lying ≈ 2 eV below the top of band (with $|m_c| < |m_v|$). These transitions corresponds to the case $-1 < g < 0$, see the inset on Fig. 1.

(2) Transitions from the lower-lying bands to the states of the band formed by Cul(d)-O1(p)-O4(p) orbitals with the top located near the FL. For these transitions, $m_c < 0$ and $|m_c| > |m_v|$ (the case $|g| > 1$, see the inset on Fig. 2a and 2b).

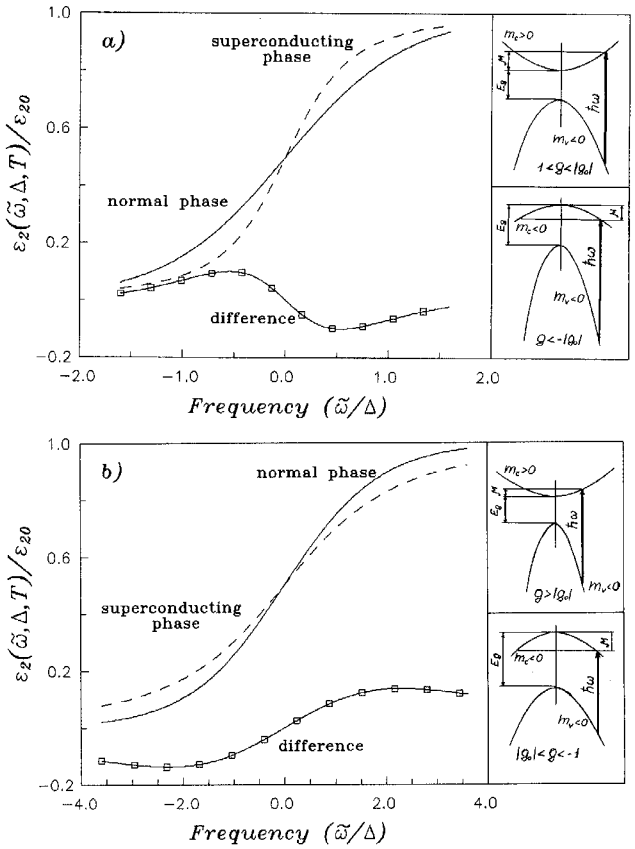

Figure 2. The imaginary part of the dielectric function, corresponding to the interband transitions in the cases a) $g = 1.2$ and b) $g = 2.5$; $\mu/\Delta \gg 1$. The dashed, solid and solid with squares lines correspond to the superconducting phase (for $\Delta = 30$ meV, $T = 63$ K), to the normal phase (for $T = 92$ K) and to the difference between them, respectively. Insets: Diagrams of interband transitions from the ligh effective mass band to the heavy effective mass band $|g| > 1$.

(3) Transitions from the lower bands to the states of above-mentioned conduction band of the heavy carriers with negative sign of the effective mass $m_c < 0$ (with $|m_c| \approx |m_v|$). This corresponds to the case $|g| \approx 1$, see the inset on Fig. 3.

Besides, the optical interband transitions with $|g| < 1$ and with $|g| > 1$ are also possible near the Γ point of BZ.

The absorption spectrum of the superconducting phase for the transitions from the heavy effective mass band to the light effective mass band (see the insets on Fig. 1.) with different effective mass sign ($-1 < g < 1$) may differ from that of the normal phase in a frequency region $\Delta\omega = \Delta\sqrt{1-g^2}$. So the feature near FL may be observed (see Fig. 1). Consider the quantity $\epsilon_2^r(\tilde{\omega}, T) = \epsilon_2(\tilde{\omega}, \Delta, T, \gamma)/\epsilon_2(\tilde{\omega} = 0, \Delta == 0, T = 0)$. The difference $\Delta\epsilon_2^r(\tilde{\omega}) = \epsilon_2^r(\omega, T_1) - \epsilon_2^r(\tilde{\omega}, T_2)$ with $T_1 > Tc$, $T_2 < T_c$ has a definite symmetry, namely, the areas relating to the curve at $\Delta\epsilon_2(\tilde{\omega} < \Delta) > 0$ and to the curve at $\Delta\epsilon_2(\tilde{\omega} > \Delta) < 0$ are equal. The curve crosses zero at $\tilde{\omega} \approx \tilde{\Delta}$. With increasing $|g| \to 1$ the width of the characteristic structure near FL is decreased.

The absorption spectrum of the superconducting phase for the transitions from the light band to the heavy band with opposite effective mass sign ($g > 1$, see the inset on Fig. 2a.) may differ from that of the norrnal phase in a frequency region $\Delta\omega = \Delta\sqrt{g^2-1}$ (Fig.2a). With increasing g, the width of the characteristic structure is increased, its amplitude is reduced. The characteristic structure reverses its sign (see Fig.2b) at $g = g_c$, which approximately is defined by the relation

$$g_c = [(2\Delta(0)/T_c)^2 + 16]/[(2\Delta(0)/T_c)^2 - 16] \qquad (3)$$

The absorption spectrum for the transitions from the light band to the heavy band with the same effective mass sign ($g < -1$) can be obtained as a specula refiection of the Fig. 2, relatively the point $\tilde{\omega} = 0$.

The difference in the absorption spectrum of the superconducting and normal phases in the case of nearly symmetric bands (see the inset on Fig. 3.) may be observed in a frequency region $\Delta\omega = \sqrt{\mu^2 + \Delta^2} - \mu$ which is small when FL is located far from the extremum point of the band ($\Delta/\mu << 1$) - of the order of $\Delta^2/2\mu$. The characteristic structure near the FL located not far from extremum point of the conducting band ($\Delta/\mu \approx 1$) may be observed in the frequency region $\sim \Delta/2$. The main contribution to the positive

part of this structure is connected with the presence of a lower-lying threshold of the absorption. The last is determined by the top of the conducting band for transitions from the light band to the heavy band with the same sign of dispersion ($g < -1$) (Fig. 3).

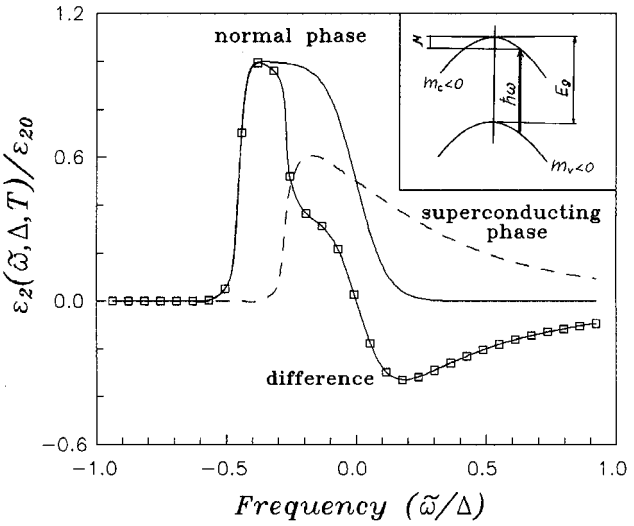

Figure 3. The imaginary part of the dielectric function, corresponding to transitions at $g = 1.1$, $\mu/\Delta \approx 2$. The dashed, solid and solid with squares lines correspond to the superconducting phase ($\Delta = 30$ meV, $T = 63$ K), to the normal phase ($T = 92$ K) and to the difference between them, respectively. Inset: The diagram of interband transitions in the case of nearly symmetric bands.

The dependencies obtained show that the cases when $|m_c/m_v| \ll 1$, $\Delta \ll \mu$ and $|m_c/m_v \approx 1$, $\Delta \leq \mu$ are the *most favorable for the experimental observation* of differences in optical properties of a material in normal and superconducting states.

The femtosecond laser spectroscopy can also be used to investigate the anisotropy of the superconducting energy gap. Recently[15] the optical properties of the model system with anisotropic order parameter

$$\Delta = \Delta_0(s + d\exp(i\beta)\cos(2\varphi))$$

were analyzed in the same framework as considered above for the pure s-wave pairing. Here s and $d(s > 0, d > 0, s + d = 1)$ are relative contributions of s-wave and d-wave pairing interactions and β is their relative phase; Δ_0 is the energy constant, depending on the temperature T.

The analysis carried out in [15] showed that not only the existence of the superconducting gap anisotropy but also s-wave and d-wave relative contributions in the superconducting order parameter may be obtained from the feature of imaginary part of the dielectric function corresponding to the transitions to the states near FL. It was shown also that the transitions between bands with $|g| \ll 1$ are the most favorable for the observation the superconducting order parameter's symmetry.

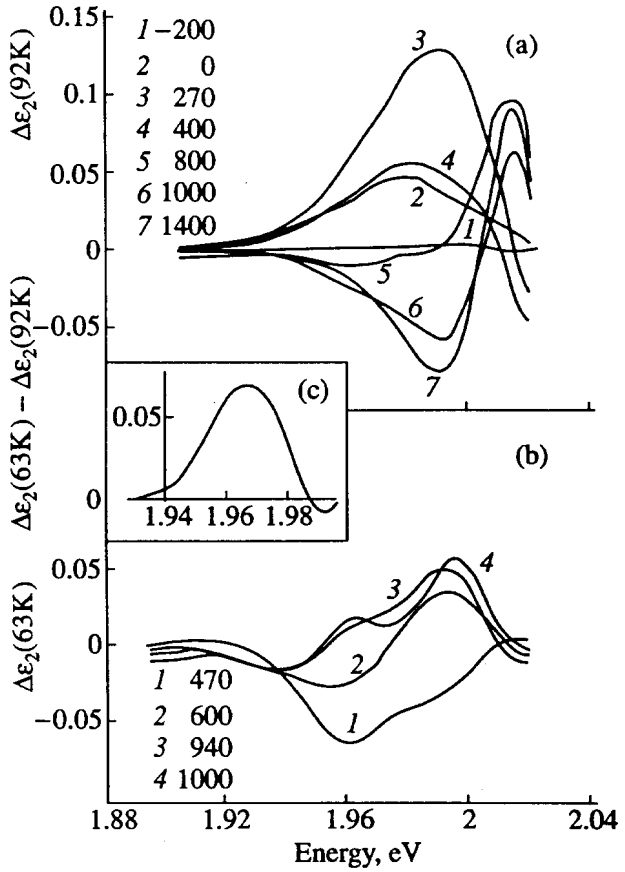

Figure 4. Difference spectra of the imaginary part of the dielectric constant e for various delays T: a) $T_0 = 92$K, b) $T_0 = 63$ K, c) the difference between spectra of $\Delta\epsilon_2$ for $T_0 = 63$ K and 92 K at long time delay (τ=1 ps) with taking into account the Fermi level shift.

IV.2. Energy gap observation[8]

To recover $\Delta\epsilon_2$ from the experimental difference transmission and reflection spectra, use was made of ellipsometric data on the equilibrium dielectric constant, $\epsilon_1(\omega)$ and $\epsilon_2(\omega)$ of $YBa_2Cu_{30}O_{7-\delta}$ [32]. The difference spectra of $\Delta\epsilon_2$ are shown in Figs. 4(a) and (b). As can be seen from the figures, the spectra for $T_0 > T_c$ also greatly differ from those for $T_0 < T_c$. At $\tau \geq 700$ fs, the spectral dependence of the response for $T_0 =$ 92 K becomes alternating: $\Delta\epsilon_2 < 0$ for $\hbar\omega < 1.99$ eV

and $\Delta\epsilon_2 \geq 0$ for $\hbar\omega \geq 1.99$ eV. Subsequently, starting from $\tau \approx 1$ ps the shape of the spectrum ceases to change - it remains alternating, with $\Delta\epsilon_2 = 0$ at $\hbar\omega = 2$ eV [Fig.4(a)]. As discussed above an alternating response is characteristic of the spectral range corresponding to transitions either into or out of the Fermi level region[5-7]. The position of the Fermi level in the spectral region $\hbar\omega \approx 2$ eV agrees with the data of Ref. [9] . The decrease of transmission (ϵ_2 rise) for short delay times over a wide spectral range [Fig.4(a)] is to all appearance due to the shift of the Fermi level as a result of strong heating of the charge carriers. The absence of any substantial changes in the $\Delta\epsilon_2$ spectrum at $\tau \geq 1$ ps points to the establishment of a quasiequilibrium. By this moment, the temperature of the sample reached 500 K, and the system loses its memory of the initial conditions, so that the difference of a mere 30 K between the initial temperatures cannot bring about any significant dissimilarities in the spectra of the excited sample. It can therefore be argued that the diversities observed in the difference spectra at $\tau > 1$ ps [see Figs.4(a) and 4(b)] can only result from the differences between the spectra of the sample in the initial (unexcited) state. This can be explained by the presence of an energy gap in the vicinity of the Fermi level for T_0 = 63 K

Subtracting the difference spectrum $\Delta\epsilon_2$ for T_0 = 92 K at $\tau = 1$ ps from that for $T_0 = 63$ K, we obtain a peak around 30 meV wide in the neighborhood of some 2 eV [Fig.4(c)]. Relating the width of this peak to the width Δ of the energy gap, we get $2\Delta_0/T_c \sim 8$, which agrees with the data reported in Ref. [33].

The presence of an energy gap in the initial state can also explain the lag of the optical response maximum observed to occur for $T_0 < T_c$ in the vicinity of the Fermi level. The magnitude of this lag ($\approx$ 200 fs) matches the time it takes for superconductivity to be destructed (see also Ref [34]).

IV.3. Temporal behavior of difference optical density spectra. [8]

Fig. 5 shows the relationship between the optical density of the difference transmission spectra of ΔD and the delay time τ for the most typical regions. The zero delay time was determined from the results of independent experiments with a serniconductor- doped glass filter RG- 8. At T_0 = 92 K (Fig. 5, curve a), the shape of the curves remains qualitatively the same throughout the spectral range of interest: ΔD is seen to decrease for a characteristic time of the order of 100 fs and then relax during < 1 ps. The difference between the curves for various regions of the spectrum is that asymptotic value of ΔD is less than zero at $\hbar\omega < 1.96$ eV and greater than zero at $\hbar\omega > 1.96$ eV. Similar curves, though relaxing to $\Delta D \approx 0$, were observed at T_0 = 70 K for $\hbar\omega < 1.93$ eV (Fig. 5, curve b). The curves for $\hbar\omega > 1.93$ eV at this temperature reversed sign (Fig.5, curve c); i.e., ΔD was first observed to increase and then relax to various asymptotic values, depending on wavelength. The relaxation of ΔD in the vicinity of $\hbar\omega = 1.98$ eV was nonmonotonic: two to three ΔD oscillations were observed to occur on a 300-500-fs scale. An essential feature of the curves obtained at $T_0 < T_c$ is the delay of the response for $\approx$ 200 fs in the region of 1. 98 eV (Fig. 5, curve c), compared to that in the region of 1.91 eV (Fig. 5, curve b) and the response at $T_0 > T_c$ (Fig. 5, curve a). The magnitude of this delay is roughly three times the relative lag of the various spectral components of probe pulse, observed to occur in the experirnent as a result of dispersion.

IV.4. The electron-phonon interaction parameter [8]

The experimental curves of Fig. 5 were used to estimate the electron-phonon interaction parameter $\lambda < \omega^2 >$ as follows. The dielectric constant of the sample varies as a result of the heating of electrons and the shifting of energy bands due to the heating of the lattice and thermoelasticity effects. Within the framework of linear response, this variation (the change of transmission in our case) can be represented in the form[35] $\Delta T_{sc} = a\Delta T_e(t) + b\Delta T_L(t)$, where $T_e(t)$ is the electron temperature and $T_L(t)$ the lattice temperature. To calculate the dynamics of ΔT_{sc}, the temporal variations of $T_e(t)$ and $T_L(t)$ were determined from the set of equations[35,36]

$$C_e\frac{\partial T_e}{\partial t} = -g(T_e,T_L)\cdot(T_e-T_L)+\frac{1}{L_{sc}}[1-R_{sc}(t)-T_{sc}(t)]\cdot I_p(t)\ ,$$
$$C_L(T_L)\frac{\partial T_L}{\partial t} = -g(T_e,T_L)\cdot(T_e-T_L)+g_{esc}(T_L,T_0)\cdot C_L\cdot(T_L-T_0) \quad (4)$$

where $R_{sc}(t)$ is the reflectivity of the multilayer system, $T_{sc}(t)$ the transmissivity of the superconductor layer, L_{sc} the superconductor layer thickness, $I_p(t)$ the pump pulse intensity, C_e and C_L are the electronic and lattice heat capacities, and $\tau_{esc}=1/g_{esc}(T_L,T_0)$ is the time it takes for phonons to escape into the substrate.

According to Allen[36], in the high temperature limit $T_e > \Theta_D$ the electron-phonon relaxation rate is described by the expression

$$g(T_e,T_L)=\pi\hbar k_B N(E_F)\lambda<\omega^2>\left[1+\frac{\hbar^2<\omega^4>}{12<\omega^2>k_B^2T_eT_L}\right]^{-1}$$
$$\lambda<\omega">=2\int_0^\infty d\omega[\alpha^2F(\omega)/\omega]\omega"$$

Here $\alpha^2(\omega)$ is the Ehashberg electron- phonon coupling function, $N(E_F)$ is the electron density of states of both spins at the Fermi level. According to the calculation results on the band structure of $YBa_2Cu_{30}O_{7-\delta}$ (Refs. [24-31]), transitions across the forbidden gap start from an energy of around 3 eV. For this reason, it can be assumed that practically all of the absorbed pump pulse energy goes to the heating of the charge carriers. This is allowed for in Eq.(4). The quantity τ_{esc} can be estimated at $>$ 10 ps. For $C_L(T_L)$, we interpolated the data reported in Refs. [37-38]. The temperature dependence for $C_e(T_e)$ can be taken from Ref. [39]. We have taken it to be $C_e(T_e)=\gamma T_e$ with γ = 16 mJ/mole*K^2 - the value, that corresponds to the density of states at the Fermi level, calculated in Refs. [24,28,29] and only slightly differs from the value of γ = 18 mJ/mole*K^2 measured in Ref. [39] for $YBa_2Cu_{30}O_{7-\delta}$ at high temperatures T_e = 300K. According to our calculation results, the maximum temperature of the charge carriers reaches some 3000 K The maximum temperature of the lattice is around 600 K The theoretical functions $\Delta T_{sc}(t)$, calculated with due regard for the Gaussian shape of the pump and probe pulses, were compared to the experimental curves (see Fig. 5). Comparison was made for the spectral range 1.91-1.95 eV far from the Fermi level in order to avoid the possible nonlinear effects associated with the shift of the level as a result of strong heating of electrons. The resultant estimate is $\lambda<\omega^2>=450\pm150$ (meV)^2. Using for $<\omega^2>$ the estimate $<\omega^2>=\Theta_D^2/2$ and taking the Debye temperature Θ_D at 350 K [37], we get the following estimate for the electron-phonon coupling constant: $\lambda=1\pm0.3$. Our data fit the results of the femtosecond pump-probe measurements[40] and the value of $\approx$1 found in Refs. [29,30] by the local density-functional method (see Table 1). Nevertheless, obtained in our experiment value of λ is somewhat lower than the value of $\approx$2 found by calculations in Refs. [31,42,43].

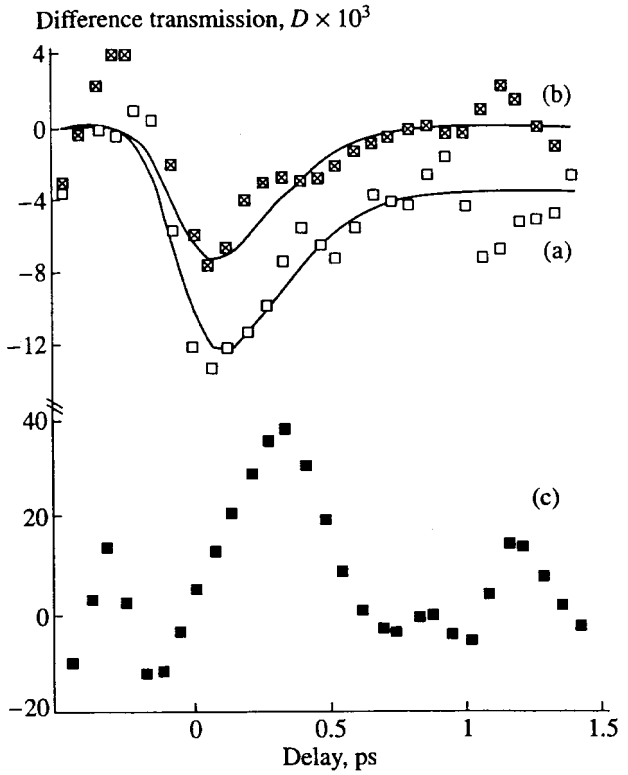

Figure 5. Difference transmission of the sample as a function of time for various energy of the probe quanta $\hbar\omega$. a) $T_0 = 92$ K, $\hbar\omega = 1.95$ eV, b) $T_0 = 70$ K, $\hbar\omega = 1.91$ eV, c) $T_0 = 70$ K, $\hbar\omega = 1.98$ eV. The solid curves are the numerical fits to the experimental data for $\lambda < \omega^2 >= 450$ $(\text{meV})^2$, $\gamma = 16$ mJ/moleK^2, and $I_p = 2 \times 10^{11}$ W/cm^2.

V. Fullerites

V.1. Introduction

The optical properties of C_{60} in the solid phase were investigated by various techniques: transmission spectroscopy of thin films[44–48], reflection spectroscopy[49], and ellipsometric measurements[50,51]. Investigation results have shown that absorption in fullerites starts in the energy range 1.6-2 eV, which is followed by a series of sharp peaks at $\hbar\omega \sim 2.7$, 3.5, 4.5, and 5.6 eV.

The numerical calculations[52–55] of the electronic structure of fullerites show a direct forbidden gap (at the X- point of the Brillouin zone) with $E_g \sim 1.7$ eV, and also indicate these bands being rather narrow (0.5-1 eV) arranged in nonoverlapping groups. The latter circumstance allows the fullerites to be classified by the representations of their molecular orbitals. According to such a classification, the upper group of valence bands forms the h_u bands and the lower group of conduction bands, the t_{lu} bands (see Fig. 6).

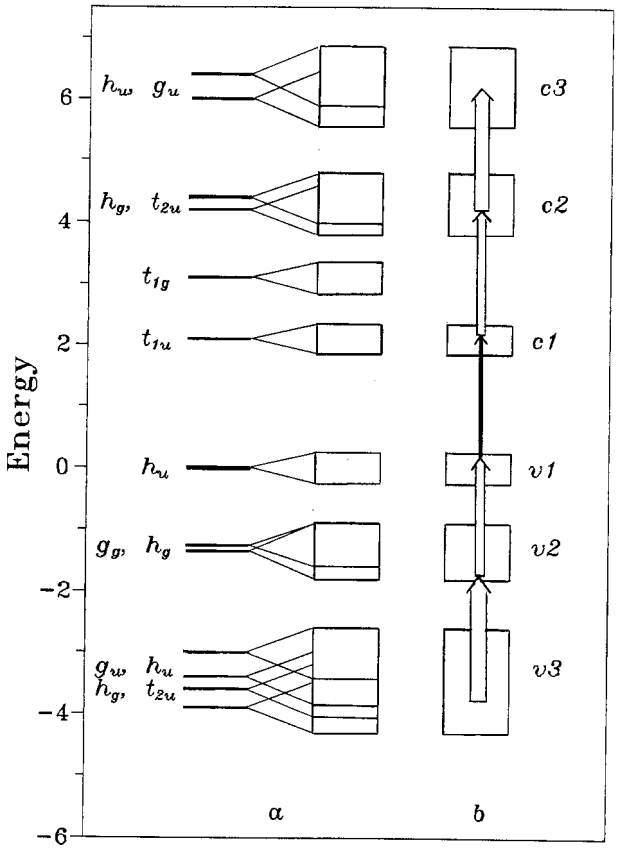

Figure 6. Energy level and optical transition diagram for fullerite: (a) splitting of molecular levels in the crystal. The lines indicate the centers of the groups of bands. The band symbols are given on the left of the lines. (b) Simplified energy band structure. One-photon transitions are shown by the arrows. The thickness of the arrow indicates the probability of corresponding transition.

The optical dipole transition $h_u \rightarrow t_{lu}$ (HOMO $\rightarrow$ LUMO transition) is forbidden in the C_{60} molecule. Weak absorption in this region results from the vibronic (Herzberg-Teller) mixing of states. In the solid phase, the mixing of states is increased owing to the crystalline field. The lowermost ($\hbar\omega \sim 3$ eV) allowed dipole transition is the $h_u \rightarrow t_{lg}$ transition. Then follow the transitions $h_g \rightarrow t_{lu}$ ($\hbar\omega \sim 3.5$ eV), $h_u \rightarrow h_g$ ($\hbar\omega \sim 4.4$ eV), and so on. It is precisely these transitions that produce strong peaks in the absorption spectra.

Studies of the fullerites' optical properties have shown that the laser excitation of a sample leads to an increase of the optical density. Femtosecond investigations[56–64] of the dynamics of fullerites' ab-

Table 1. Electron-phonon coupling constant λ and Hopfield-McMillan parameter $\lambda < \omega^2 >$ for $YBa_2Cu_{30}O_{7-\delta}$.

$\lambda < \omega^2 >$ [meV^2]	$< \omega^2 >^{1/2}$ [K]	λ	Source
		1.3 ± 1	W. Weber, L.F. Mattheiss. Phys. Rev. **B37**(1), 599 (1988)
472	440	0.32	P.B. Allen, W.E. Pickett, H. Krakauer, Phys. Rev. **B37**(13), 7482 (1987)
477	247	1.05	J. Yu, S. Massidda, A.J. Freeman, D.D. Koeling. Phys. Lett. **A122**, 203 (1987); S. Massidda, J. Yu, K.T. Park, A.J. Freeman. Physica **C176**, 159 (1991)
475±30	267	0.9 ± 0.2	S.D. Brorson, A. Kazeroonian, D.W. Face, T.K. Cheng, et al. Sol. State Comm. **74**(12), 1305 (1990)
		1	O.K. Andersen, A.I. Liechtenstein, O. Rodriguez, I.I. Masin et al. Physica **C185-189**, 147 (1991)
450± 150	247	1 ± 0.3	S.V. Chekalin, V.M. Farztdinov, V.V. Golovlev, V.S. Letokhov et al. Phys. Rev. Lett. **67**, 3860 (1991)
		1.7±1.0	I.I. Mazin, O. Jepsen, O.K. Andersen, S.N. Rashkeev, Yu.A. Uspensky. Phys.Rev. **B45**, 5103 (1992)
∼2200		1.95	G.L. Zhao, J. Callaway. Phys. Rev. **B49**(9), 6424 (1994)
		2.	R. Zeyher. J. Supercond. **7** (3), 537 (1994)

sorption revealed that the time of an increase of the optical density is pulse-width limited. The photodarkening occurs in the spectral region $\hbar\omega$ = 1.6 - 2.4 eV [58,62-64]. This energy region in the ground-state spectrum[44-51] corresponds to the $h_u \rightarrow t_{lu}$ transitions (dipole-forbidden for C_{60} molecules) from an upper group of valence bands to a lower group of conduction bands (see Fig. 6).

V.2. The spectral and temporal behavior of the optical density [62-64].

V.2.1. Experimental results

The results obtained from femtosecond laser spectroscopy investigations[62-64] show that in the spectral range 1.8-2.3 eV the sample suffered darkening caused by the exciting pulses. The amount of darkening at a fixed delay of the probing pulse relative to its exciting counterpart was found to depend on the probing pulse energy, reaching its maximum in the neighborhood of $\hbar\omega \sim 2.25$ eV. The position of maximum agrees with one on the experimental absorption spectrum in Ref. 58.

Typical temporal behavior curves of the optical density ΔD are presented in Fig. 7. While studying the dependence of ΔD on the exciting pulse intensity, we found that increasing the intensity caused a proportional increase in the height of the peak at zero delays (see Fig. 8). The shape of the peak at high intensities can be described well enough by the autocorrelation function of the exciting pulse. Such behavior of the peak at zero delays gives reason to believe that it is associated with two-photon from the ground and the excited states.

Approximating the experimental dependences $\Delta D_{\rm exp}(t)$ by the theoretical functions $\Delta D_{\rm theor}(t)$ with due regard for the contribution to absorption from two- photon transitions, we obtained the following optical density relaxation rates: $\gamma_1 \approx 1.3 \pm 0.3$ ps^{-1} ($\tau_1 \approx 800 \pm 200$ fs) and $\gamma_2 \approx 0.03$ ps^{-1} ($\tau_2 \approx 30$ ps). Accurate to within the determination error of τ_1 we have found τ_1 to be independent of probing pulse energy $\hbar\omega$ and of pumping pulse intensity.

We get also the following estimate of the two-photon absorption coefficient β (at a probing photon energy of $\hbar\omega = 1.88$ eV): $\beta \sim 2 \times 10^{-8}$ cm/W ($Im\chi^{(3)} \sim 2.10^{-11}$ esu).

The value obtained for τ_1 agrees well with the value of $\tau_1 \sim 900$ fs obtained in Ref. [60] for an intensity of around 10^{11} W/cm^2.

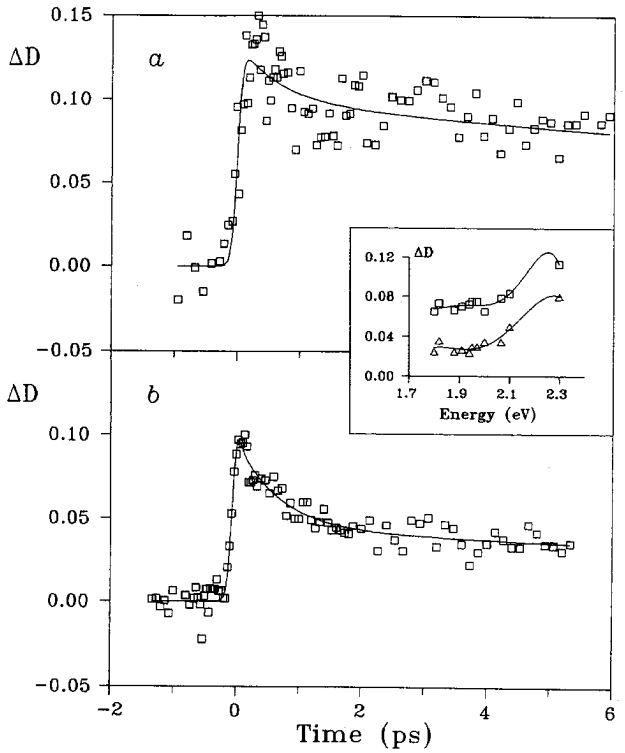

Figure 7. Time dependence of the optical density variation $\Delta D(t)$ for intensity $I \approx 1 \times 10^{11}$ W/cm^2: (a) at a photon energy of $\hbar\omega = 2.3$ eV; (b) at a photon energy of 1.82 eV. The inset shows optical density variation spectra at delay times of 0.5 ps (□) and 4 ps (Δ). The fitting lines were drawn to have a peak in the same energy region as in our separate measurements of the optical density spectra at different positive time delays (not shown in the figure).

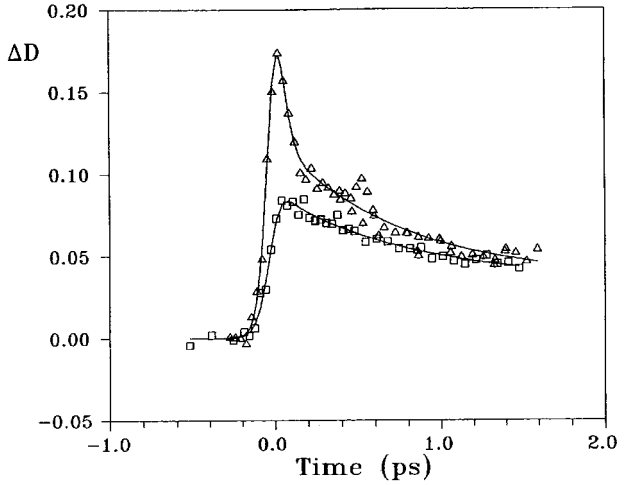

Figure 8. Time dependence of optical density variation $\Delta D(t)$ at a photon energy of $\hbar\omega = 1.88$ eV for various intensities: (□)$I \approx 10^{11}$ W/cm^2; (Δ) – $I \approx 2 \times 10^{11}$ W/cm^2.

V.2.2 Physical causes of photodarkening

Consider the physical causes of increased absorption in fullerites. The spectral region studied corresponds to transitions from the upper group of valence bands to the lower group of conduction bands, ie., to the $h_u \rightarrow t_{lu}$ transitions in Fig. 6. The filling of states in the t_{lu} group of bands, under the effect of the exciting pulse, makes possible dipole transitions from the lower group of conduction bands to higher bands, the $t_{lu} \rightarrow h_g$ transitions in Fig. 6. Absorption for these transitions (see Refs. [52-55,65-66]) fall within the $\hbar\omega$ region of 2.2 ± 0.45 eV, i.e., within the spectral region under study. Such an increased absorption should also be caused by the depletion of states in the h_u group of bands, allowing dipole transitions from the group of valence bands $h_g + g_g$ to unfilled states in the h_u group of valence bands (see Fig. 3). Absorption for these transitions falls within the $\hbar\omega$ region around 1.4 ± 0.6 eV [52- 55,65-66]; i.e., it overlaps with the spectral region being studied.

Another cause of increased absorption may be the growth of the dipole moment operator matrix element for the $h_u \rightarrow t_{lu}$ transitions. This may result from the increase in the mixing of the t_{lu} and t_{lg} states (and h_u and h_g states) caused by the excitation of the a_u, t_{lu}, h_u and a number of other odd intramolecular vibrations upon the absorption of the exciting pulse. This should increase the absorption coefficient in the $\hbar\omega$ region in the vicinity of 1.9 ± 0.45 eV.

The increase of absorption as a result of transitions from the excited state can be distinguished from that due to the increased vibronic mixing of states by the differences in the temporal behavior of absorption in these two cases. Indeed, in the first case, in the spectral region under study, the fast rise of absorption caused by the filling of states in the bands with hot charge carriers is followed by a slight reduction of absorption occurring on the scale of the characteristic electronic-vibrational relaxation time. This results from the arrangement of the energy bands in the crystal phase of C_{60} and is associated with the fact that as the hot carriers cool off, they go from states corresponding to higher absorption coefficients to those characterized by lower absorption coefficients (for the wavelength range under study). In the second case, absorption increases as a result of the excitation of the a_u, t_{lu}, h_u, and some other odd intramolecular vibrations upon the absorption of the exciting pulse. Absorption then rises slowly on account

of the anharmonic decay of the a_g and h_g intramolecular vibrations, which are excited in the course of the energy relaxation of the charge carriers, to the t_{lu}, t_{2u}, g_u, and h_u vibrations on the scale of the characteristic phonon-phonon interaction time. The non-totally symmetric vibrations h_g may also lead to the broadening (splitting) of the t_{lu} bands as a result of the Jahn-Teller effect.

The spectral temporal behavior of optical density points to the fact that the main contribution to absorption variation comes from the filing of electronic states and the depletion of hole states in the t_{lu} and h_u bands, respectively. The temporal dynamics is due to the relaxation of the free charge carriers interacting with intra- and intermolecular vibrations (phonons). Initially, both high-frequency intramolecular vibrations, a_g and h_g, and low-frequency intermolecular vibrations (lattice phonons) are excited. The cooling of the carriers will cause the filling of states near the bottom of the conduction band by electrons and those near the top of the valence band by holes. When the energy of the charge carriers proves insufficient to excite intramolecular vibrations, the main relaxation mechanism is the generation of optical lattice phonons. Accordingly, the characteristic relaxation time should grow substantially longer, which was exactly what was observed to occur in our experiments.

The absorption peak observed at zero delays between the exciting and probing pulses is apparently due to two-photon (multiphoton) absorption. This hypothesis is based on the fact that the height of this peak grows with the increasing intensity, and its shape is described well enough by the autocorrelation function of the exciting pulse.

In accordance with the arrangement of bands in crystalline C_{60} (see Fig. 6), the $h_g \to t_{lg}$ and $h_u \to t_{2u}$ two-photon transitions are possible in the $\hbar\omega$ region around 2 eV. To our view, the main contribution is from the $h_g \to t_{lg}$ transitions. In the excited state (when states in the h_u band get depleted), new channels are opened up for two- photon transitions: $H_g + g_g \to t_{lg}$ via the intermediate state h_u.

The study of the optical density dependence on the exciting pulse intensity revealed[47,58,62,63] that increasing the intensity caused a proportional increase in the amount of darkening at low excitation energy levels. Recently it was found experimentally in Refs. 58, 62 and 63 that for high excitation energy levels the increase of darkening saturates. Here the question arises: What is the reason of the darkening saturation? Is it a process inherent to photodarkening itself or a consequence of some new phenomenon?

V.3. Saturation of the fullerite photodarkening. Theory [73]

Consider the temporal variation of the optical density of a C_{60} film in the spectral range 1.6 - 2.4 eV (range of $h_u \to t_{lu}$ transitions in the ground state) and the dependence of this density on the laser energy fluence. The sample is taken to be excited by the optical pulses with a duration of some 100 fs (or shorter) and a photon energy of $\hbar\omega \approx 2$ eV (typical value for the most of recent pump-probe experiments[56-64]).

To obtain a theory that *qualitatively* correctly describes energy fluence dependence of the optical density we will neglect the effects of inter- and intraband electron-phonon relaxation of charge carriers. We will be interested only in time-delays that are substantially shorter than the characteristic interband relaxation times.

V.3.1. Description of the model

The complicated energy band structure of fullerite (see, for example, Refs. [52-55] for its numerical calculations and Refs. [44-51,65-70] for its experimental investigations by different methods) can be replaced by the following one: the lower valence band v3 (corresponds to g_u, h_u, t_{2u} valence bands), the valence band v2 (corresponds to h_g, g_g bands), the upper valence band v1 (corresponds to the h_u bands), the lower conductivity band c1 (corresponds to t_{lu} bands), the conductivity band c2 (corresponds to the t_{2u} and h_g conductivity bands), the upper conductivity band c3 (corresponds to the h_u and g_u conductivity bands). The compatibility between the supposed energy band structure and that of crystalline C_{60} is shown in Fig. 6.

The distance between the band centers is following[52-55,65-70]: $v3 \leftrightarrow v2 = 2$ eV, $v2 \leftrightarrow v1 = 1.4$ eV, $v1 \leftrightarrow c1 = 2.1$ eV, $c1 \leftrightarrow c2 = 2.2$ eV, $c2 \leftrightarrow c3 = 1.9$ eV. Because of the bands are of width of 0.5 eV [52-55, 65-70], the single-photon transitions with energy $\hbar\omega \sim$

2 eV are possible between each pair of bands. For the same reason the exact value of the energy gap is of little consequence for our consideration.

The absorption coefficients dependence on the band filling are considered in the approximation of a uniform distribution of charge carriers over all states in each band. Only time delays that are shorter than electron- phonon energy relaxation time are considered; as a measure of this time a value of ~1 ps, obtained in the experiments[62,64,66,67], can be used.

The number of states n_{10} in the band c1 is taken to be equal to the number of states in v1 band (the ratio of their real values is 0.7). An analogous relation is assumed to hold for bands c2 and v2. Their real ratio here is 0.9. The number of states n_{20} in the c2 band is greater than that in the c1 band: $\eta = n_{10}/n_{20} \approx 0.4 < 1$.

According to the discussion in the previous paragraph the absorption coefficients α_{v1} and $c1$ for the transitions $v2 \leftrightarrow v1$ and $c1 \rightarrow c2$ are greater than the absorption coefficient α_0 for the transitions $v1 \rightarrow c1$. For simplicity the we presumed that $\alpha_{v1} = \alpha_{c1} = \alpha_1 > \alpha_0$. The same were also supposed for the absorption coefficients α_{v2} and α_{c2} (for transitions $v3 \rightarrow v2$ and $c2 \rightarrow c3$ respectively): $\alpha_{v2} = \alpha_{c2} = \alpha_2$. Insofar as transitions $v3 \rightarrow v2$ and $c2 \rightarrow c3$ are also dipole-allowed, the α_2 is of the same order of magnitude as α_1. Relying on the femtosecond experiment data[61], one can even suppose that $\alpha_2 > \alpha_1$.

As discussed above the two-photon absorption is governed by $h_g \rightarrow t_{lg}$ transitions. These transitions change the carrier density only in the v2 band. For the excitation energy fluences under consideration the filling of states in v2 band by holes, generated as a consequence of such transitions, is of little importance and its influence was ignored. At the same time the contribution of two-photon transitions to the total absorption was accounted for.

V.3.2 Energy fluence dependence of the optical density

The optical density variation of the thin film sample ($D_0 \ll 1$) in the pump-probe experiment can be described by the expression

$$\frac{\Delta D(t)}{D_0} = \frac{\Delta\alpha(t)}{\alpha_0} + \frac{\beta}{\alpha_0} \cdot I_p(t) \ ,$$
$$D_0 = \alpha_0 = \cdot L_{\rm film} \cdot log_{10}(e) \ .$$

where $\Delta\alpha(t)$ is the change of one-photon absorption coefficient, β is the two-photon absorption coefficient, $I_p(t)$ is pumping pulse intensity in the film of thickness $L_{\rm film}$, and t is a time-delay between pumping and probing pulses. Consider the variation of charge carriers under the influence of laser pulses with intensity $I_p(t) = E_p \cdot f(t)$, where E_p is excitation energy fluence, and $f(t)$ is pulse shape function normalized so that $F(t) = \int_{-\infty}^{t} dt' f(t')$, $F(+\infty) = 1$. The specific pulse shape is of no importance for our purposes here. It may be described, for example, by the function $f(t) = (1/2\tau_p) \cdot cosh^{-2}(t/\tau_p)$.

By introduction of the parameter $\beta_s = \beta \cdot \hbar\omega_p \cdot n_{10}/\alpha_0^2$, the expression for the optical density temporal variation can be presented in the following form

$$\frac{\Delta D(t)}{D_0} = 2\left(\frac{\alpha_1 - \alpha_0}{\alpha_0}\right)\nu_1(t) + 2\left(\frac{\alpha_2 - \alpha_1}{\alpha_0}\right)\nu_2(t) + \beta_s \cdot N_0 \cdot f(t) \qquad (5)$$

Here the values ν_1 and ν_2 are band filling fractions, $N_0 = \alpha_0 E_p/(\hbar\omega_p \cdot n_{10})$ is proportional to the density of photons.

$$\nu_1(t) = \frac{1}{\Delta} \cdot \left\{ \left[1 - \frac{\eta}{\lambda_1}\frac{(\alpha_1 + \alpha_2)}{\alpha_0}\right] \cdot \Theta_1(t) - \left[1 - \frac{\eta}{\lambda_1}\frac{(\alpha_1 + \alpha_2)}{\alpha_0}\right] \cdot \Theta_2(t) = \right\}$$
$$\nu_2(t) = \frac{\eta}{\Delta} \cdot \frac{\alpha_1}{\alpha_0}\left\{\frac{1}{\lambda_2} \cdot \Theta_2(t) - \frac{1}{\lambda_1} \cdot \Theta_1(t)\right\} \qquad (6)$$

where we have introduced following notations

$$\Delta = [(2|\alpha_1/\alpha_0 - \eta(\alpha_1 + \alpha_2)/\alpha_0)^2 + 4\eta(\alpha_1/\alpha_0)^2]^{1/2}$$

$$\lambda_{1,2} = \frac{1}{2}[2 + \alpha_1/\alpha_0 + \eta \cdot (\alpha_1 + \alpha_2)/\alpha_0 \pm \Delta] \ , \ \Theta_{1,2}(t) = [1 - \exp(-\lambda_{1,2} N_0 F(t))]$$

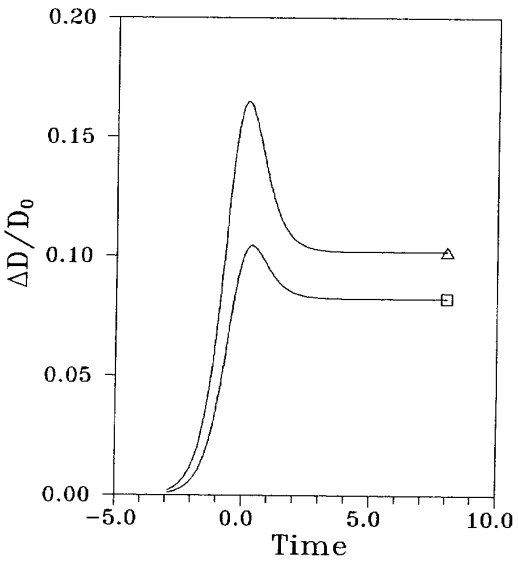

Figure 9. Time dependence of optical density variations $\Delta D(t)$ for various energy fluences: (□) $N_0 = 1$; (△) $N_0 = 2$. Time is in units of τ_p; $\beta_s = 0.04 \times 2\tau_p$. The parameters used are the following: $\alpha/\alpha_0 = 1.1$, $2/a_0 = 1.2$, $\eta = 0.5$.

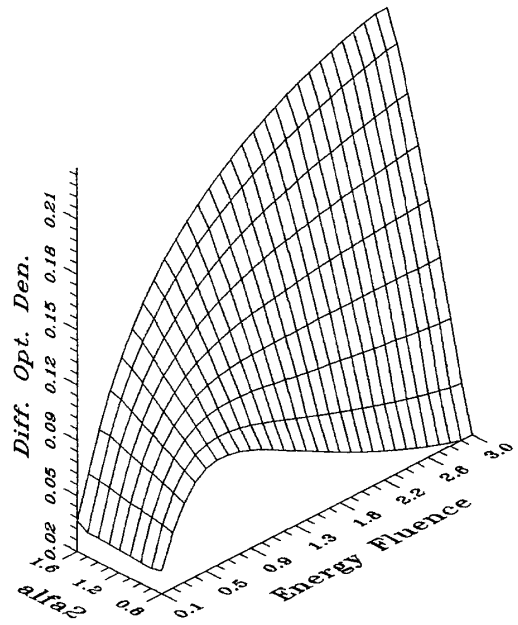

Figure 10. The exciting energy dependence of the difference optical density $\Delta D(t = 3\tau_p)$ after pumping pulse passage. The parameters used are following: $\alpha_1/\alpha_0 = 1.2$, $\eta = 0.5$. Energy fluence is in dimensionless units.

The temporal dependencies (5) for different excitation energy levels are depicted in the Fig. 9. The dependence of $\Delta D/D_0$ on the energy fluence at delays $t > \tau_p$ is shown in the Fig. 10. The qualitative view of these curves is weakly sensitive to the choice of parameters $\alpha_1 \approx \alpha_2, \eta$, and $\beta_s - \Delta D/D_0$ increases with energy fluence at first linearly, and then the slowdown of the increase is observed.

V.3.3. Discussion

As is obvious from the expression (5) and Fig. 9, for the time-delays $t > \tau_p$ at low exciting energy fluences E_p (when $N_0 \ll 1$) the optical density increases almost linearly as the energy fluence is raised. At high exciting energy fluences (when $N_0 \sim 1$) the optical density dependence versus intensity becomes weak. Both effects - quick increase at $N_0 \ll 1$ and slow one at $N_0 \sim 1$ are the consequence of the fact that the absorption coefficient al in the excited state has the higher value than the absorption coefficient α_1 in the ground state.

The derived dependence of the optical density on the energy fluence agrees well with the experimental findings in Refs. 62 and 63. The slowdown of the increase of the optical density at zero time delay was observed in Ref 58. The diminishing of the increase of inverse self-transmission coefficient at high energy iluences was observed in Ref 71.

The behavior of the optical density, predicted by our model differs significantly from that anticipated from the increase of the oscillator strength of $h_u \rightarrow t_{lu}$ transitions. In former case the *saturation of darkening* occurs at high exciting energy fluences $N_0 \sim 1$, while in the latter case there would be *total bleaching* at such energy fluences. Furthermore, the temporal behavior of these effects is quite different (see preceeding paragraph for detailed discussion).

The saturation of darkening is attended with charge carriers redistribution between bands. Initially, at $N_0 \ll 1$, the fast increase of the density of electrons and holes takes place in the bands c1 and v1 respectively. When N_0 is further increased the electrons from deeply lying valence bands are transferred to the upper conductivity bands due to multi-step transitions

- at first the carriers density is increased in bands c2 and v2, then it increases in the bands c3 and v3. The ground state ionization potential of solid C_{60} is of 7.6 eV [67,69] . Therefore the ionization of C_{60} crystal can occur from the band c3 upon the absorption of another photon (with energy $\hbar\omega \sim 2$ eV). The ionization process is similar to multi-step ionization of molecules, discussed at length in Ref. 72. Recently the effective ionization of solid C_{60} by femtosecond optical pulses on the wavelength of 620 nm was found experimentally[74].

As is seen from Fig. 6, the transitions $v2 \rightarrow v1$ will be accompanied by a strong heating of charge carriers. Therefore, an increase of laser energy density will lead to a rise of carriers temperature. The higher the carriers temperature, the easier they emit the highest frequency intramolecular vibrations and the faster they lose the energy. This effect may be at least in part the reason of the decrease of the relaxation time, observed in Refs. [58-60] when the energy fluence was increased.

As pointed out above, the transfer of electrons from deeply lying valence bands into the upper conductivity bands will occur in crystalline C_{60} at high excitation levels. As a result of the carriers redistribution, the luminescence, taking place on a time scale of recombination times much longer than the pulse duration, will be observed in a wide spectral range - from ~0.2 eV to ~ 5 eV. The luminescence spectrum will feature a pronounced temporal dependence. It will evolve into the peak around $\hbar\omega \approx E_g$ in an interband recombination time.

VI. Conclusions

Femtosecond laser spectroscopy was used to investigate the temporal behavior of optical spectra of high temperature superconductor $YBa_2Cu_{30}O_{7-\delta}$ and fullerite.

The femtosecond charge carrier dynamics of reflection and trasmission spectra of an $YBa_2Cu_{30}O_{7-\delta}$ film have been studied in the wavelength range 620 - 680 nm at the initial temperature both below and above the critical temperature T_c. Based on experimental data, the electron-phonon interaction parameter $\lambda < \omega^2 >$ has been estimated at 450 ± 150 $(\text{meV})^2$. We have shown that the difference optical spectra for a superconductor in the range of interband transitions into the FL region have a feature which is connected with the superconducting gap Δ.

It has been shown that the most favorable situations for experimental observation of the differences in the optical spectra between normal and superconducting phases are the situations when $|m_c/m_v| \ll 1$, $\Delta \ll \mu$ and $|m_c/m_v| \approx 1$, $\Delta \leq \mu$. It is the last case that corresponds to the interband transitions of oxide superconductor $YBa_2Cu_{30}O_{7-\delta}$ we have studied experimentally.

The temporal variation of the optical density of a C_{60} film over a wide spectral range - from 1.8 to 2.3 eV, along with its dependence on the exciting pulse intensity in the region of $\sim 10^{11}$ W/cm^2 has been experimentally studied. The spectral-temporal behavior of the optical density points to the fact that the main contribution to absorption variations comes from the filling of electronic states and the depletion of hole states in the t_{1u} and h_u bands, respectively. The temporal dynamic is due to the relaxation of the free charge carriers interacting with intra- and intermolecular vibrations (phonons). The main contribution to the carrier relaxation occurring at the first stage with a characteristic time of $\tau_1 \approx 800 \pm 200$ fs is from the intramolecular vibrations. The main relaxation mechanism on the second stage is the generation of optical lattice phonons with a characteristic time of $\tau_2 \approx 30$ ps. At an exciting pulse intensity of $I \sim 10^{11}$ W/cm^2, two-photon transitions start contributing to the total absorption. The two-photon absorption coefficient value has been estimated at some 2×10^{-8} cm/W.

It was shown theoretically that both the increase of absorption at low excitation energy levels and the saturation of this increase at high excitation energy levels are the consequence of the same effect - the higher value of absorption coefficient in the excited state. At high excitation levels multi-step ionization of C_{60} was predicted.

Acknowledgment

The work was partially supported by the grants of Russian Fundamental Research Foundation, International Science (Soros) Foundation and Scientific Program "Fullerenes and Clusters" of Russian Ministry of Sciences. We are indebted to our colleagues S.V. Chekalin, A.L. Dobryakov, V.V. Golovlev, A.G.

Stepanov, A.P. Yartsev, and V.S. Letokhov for cooperation. One of the authors (V.M.F.) would like to express his gratitude to Profs. C.H. Brito Cruz, J.I. Bigot and K. Duppen for valuable discussions of some of the problems considered here during the Adriatico Research Conference on "Ultrafast Phenomena and Applications" in Trieste, Italy (December 1994).

References

1. W. Kaiser, ed. *Ultrashort Laser pulses and Applications*; Springer: Berlin, 1988.
2. Ultrafast Phenomena VIII, Springer Series in Chem. Phys., **55**, 81 (1992).
3. N.V. Zavaritskii Usp. Fiz. Nauk **160**, 177 (1990).
4. R.W. Schoenlein, W.Z. Lin and J.G. Fujimototo, Phys. Rev.Lett. **58**, 1680 (1987).
5. G.L. Eesley, Phys.Rev. B**33**, 2144 (1986).
6. S.D. Brorson, A. Kazeroonian, J.S. Moodera, D.W. Face, T.K Cheng, E.P. Ippen, M.S. Dresselhaus and G.Dresselhaus, Phys. Rev. Lett. **64**, 2172 (1990).
7. M.E. Gershenson, V.V. Golovlev, I.B. Kedich, V.S. Letokhov, Yu.E. Lozovik, Yu. A. Matveets, E.G. Sil'kis, A.G. Stepanov, V.D. Titov, M.I. Faley, V.M. Farztdinov, S.V. Chekalin and A.P. Yartsev, Pis'ma Zh. Eksp. Teor. Fiz. **52**, 1189 (1990).
8. S.V. Chekalin, V.M. Farztdinov, V.V. Golovlev, V.S. Letokhov, Yu.E. Lozovik, Yu.A. Matveets, A.G. Stepanov, Phys. Rev. Lett. **67**, 3860 (1991).
9. S.D. Brorson, A. Kazeroonian, D.W. Face, T.K. Cheng, G.L. Doll, M.S. Dresselhaus, G. Dresselhaus, E.P. Ippen, T. Venkatesan, X.D. Wu and A. Inam, Solid State Commun. **74**, 1305 (1990).
10. S.G. Han, Z.V. Vardeny, K.S. Wong, O.G. Symko and G. Koren, Phys. Rev. Lett. **65**, 2708 (1990).
11. E.P. Ippen and C.V. Shank, in *Ultrashort Light Pulses*, edited by S.I. Shapiro (Springer-Verlag, Berlin, 1984), Chap. 3, p. 83.
12. A. Kazeroonian, T.K. Cheng, S.D. Brorson, Q. Li E.P. Ippen, X.D. Wu, T. Venkatesan, S. Etemad and G.Dresselhaus, Solid State Commun. **78**, 95 (1991).
13. A.L. Dobryakov, V.M. Farztdinov, Yu.E. Lozovik, Phys. Rev. B**47**(N 17), 11515 (1993).
14. A. L.Dobryakov, V.M. Farztdinov, Yu.E. Lozovik and V.S. Letokhov. Opt. Com **105**, 309 (1994).
15. Yu.E. Lozovik, A.V. Poushnov. Phys. Lett. A**194**, 405 (1994).
16. P. Monthoux, A. Balatsky and D. Pines. Phys. Rev. Lett. **67**, 3448 (1991).
17. N. Bulut, D.J. Scalapino. Phys. Rev. Lett. **67**, 2898 (1991).
18. Z.-X. Shen, D.S. Dessau, B.O. Wells, et. al. Phys. Rev. Lett. **70**, 1553 (1993).
19. W. Hardy, D.A. Bonn, D.C. Morgan, et al. Phys. Rev. Lett. **70**, 3999 (1993).
20. J. Liu, Y. Li, Ch. Lieber. Phys. Rev. B**49**, 6234 (1994).
21. T. E. Mason, G. Aeppli, S. M. Hayden, et.al. Phys. Rev. Lett. **71**, 919 (1993).
22. D. Chaudhari and Shaw-Yu Lin. Phys. Rev. Lett. **72**, 1084 (1994).
23. D.C. Mattis and J. Bardeen. Phys. Rev. **111**, 412 (1958).
24. S. Massidda, J.Yu. Freeman, D.D. Koeling, Phys. Lett. A**122**, 198 (1987).
25. G.-L. Zhao, Y. Xu, W.Y. Ching, K.W. Wong, Phys. Rev. B**36**, 7203 (1987).
26. P.B. Allen, W.E. Pickett, H. Krakauer, Phys. Rev. B**37** (13), 7482 (1987).
27. W.E. Pickett, R.E. Cohen, H. Krakauer, Phys. Rev. B**42**, 111, (1988).
28. W.E. Pickett, Rev. Mod. Phys. **61**, 433 (1989).
29. J. Yu, S. Massidda, A.J. Freeman, D.D. Koeling, Phys. Lett. A**122**, 203 (1987); S. Masidda, J. Yu, K.T. Park, A.J. Freeman, Physica C**176**, 159 (1991).
30. O.K. Andersen, A.I. Liechtenstein, O. Rodriguez, I.I. Masin et al. Physica C**185-189**, 147 (1991).
31. G.L. Zhao, J. Callaway. Phys. Rev. B**49**(9), 6424 (1994).
32. A. Bjorneklett, A. Borg, O. Hunderi, Physica (Amsterdam) A**157**, 164 (1989).
33. Y.M. Imer, F. Pattney, B. Dardel, W.-D. Schneider, Y. Baer, Y. Petroff and A. Zettl, Phys. Rev. Lett. **62**, 336 (1989); J. Shutzmann, W. Ose, J. Keller, K.F. Ronk, B. Roas, L.Shulz and G. Saeman-Ischenko, Europhys. Lett.**8**, 679 (1989); R.T. Collins, Z. Schlesinger, F. Holzberg and C. Freidl, Phys. Rev. Lett. **63**, 422 (1989); B.N.J.

Person, J.E. Demuth, Phys. Rev. B**42**, 8057 (1990).

34. G.L. Eesley, J. Herernanse, M.S. Meyer, G.L. Doll and S.H. Liou, Phys. Rev. Lett. **65**, 3445 (1990).
35. S.D. Brorson, A. Kazeroonian, J.S. Moodera, D.W. Face, T.K. Cheng, E.P. Ippen, M.S. Dresselhaus and G. Dresselhaus, Phys. Rev. Lett. **64**, 2172 (1990).
36. P.B. Allen, Phys. Rev. Lett. **59**, 1460 (1987).
37. K.A. Kvavadze, D.D. Igitkhanishvili, M.M. Nadareishvili, L.A. Takhnishvili, G.A. Zinzadze and M.Y. Chubabriya, Sverkhprovodimost' **3**, 1628 (1990) (in Russian).
38. M.V. Nevitt, G.W. Crabtree and T.E. Klippert, Phys. Rev. B**36**, 2398 (1987).
39. J.W. Loram, K.A. Mirza, J.R. Cooper, W.Y. Liang, Phys. Rev. Lett. **67**(11), 1740 (1993).
40. S.D. Brorson, A. Kazeroonian, D.W. Face, T.K. Cheng, G.L. Doll, M.S. Dresselhaus, G. Dresselhaus, E.P. Ippen, T. Venkatesan, X.D. Wu and A.Inam, Solid State Comm. **74**,1305 (1990); A. Kazeroonian, T.K. Cheng, S.D. Bronson, Q. Li, E.P. Ippen, X.D. Wu, T. Venkatesan, S. Etemad, M.S. Dresselhaus, G. Dresselhaus, Solid State Comm. **78**, 95 (1991).
41. I.I. Mazin, O. Jepsen, O.K. Andersen, S.N. Rashkeev, Yu.A. Uspensky, Phys. Rev. B**45**, 5103 (1992).
42. W.W. Fuller-Mora, S.A. Wolf, V.Z. Kresin, J. Supercond. **7**(3), 543 (1994).
43. R. Zeyher. J. Supercond. **7**(3), 537 (1994).
44. A. Skumanich, Chem. Phys. Letters, **182**, 486 (1991).
45. C. Reber, L. Yee, J. McKiernan, J.L. Zink, R.S. Williams, W.M. Tong, D.A.A. Ohlberg, R.L. Wetten and F. Diederich. J. Phys. Chem. **95**, 2127 (1991).
46. A.F. Hebard, R.C. Haddon, R.M. Fleming, A.R. Kotran, Appl. Phys. Letters, **59**, 2109 (1991).
47. K. Pichler, S. Graham, O.M. Gelsen, R.H. Friend, W.J. Romanow, J.P. McCauley Jr., N. Coustel, J.E. Fischer and A.B. Smith, J. Phys. C**3**, 9259 (1991).
48. W. Zhao, T.N. Zhao, J.J. Yue, L.Q. Chen, L.Q. Liu, Solid State Commun. **84**, 323 (1992).
49. P.N. Saeta, B.I. GTeen, A.R. Kotran, N. Kopylov and F.A. Thiel, Chem. Phys. Letters, **190**, 184 (1992).
50. S.L. Ren, Y. Wang, A.M. Rao, E. Mc Rae, J.M. Holden, T. Hager, Kai- An Wang, Wen-Tse Lee, H.F. Ni J. Selegue and P.C. Eklund, Appl. Phys. Letters, **59**, 2678 (1991).
51. M.K KeMy, P.Etchegoin, D.Fuchs, W. Krätschmer and K. Fostiropoulos, Phys. Rev. B**46**, 4963 (1992).
52. S. Saito and A. Oshiyama, Phys. Rev. Letters, **66**, 2637 (1991); S. Saito, Nonlinear Optics, **4**, 51 (1993).
53. S.C. Erwin, W.E. Pickett, Science, **254**, 842 (1991).
54. W.Y. Ching, M.-Z. Huang, Y.-N. Xu, W.G. Harter and F.T. Chan, Phys. Rev. Letters, **67**, 2045 (1991).
55. M.-Z. Huang, Y.-N. Xu, W.Y. Ching, J. Chem. Phys. **96**, 1648 (1992).
56. R.A. Cheville, N.J. Halas, Phys. Rev. B**45**, 4548 (1992).
57. M.J. Rosker, H.O. Marcy, T.Y. Chang, J.T. Khoury, K Hansen and R.L. Whetten, Chem. Phys. Letters, **196**, 427 (1992).
58. T.N. Thomas, J.F. Ryan, R.A. Taylor, D. Mihailoviz, R. Zambony, Int. J. Mod. Phys. B**6**, 3931 (1992). T.N. Thomas, R.A. Taylor, J.F. Ryan, D. Mihailovic and R. Zamboni , Europhys. Lett. **25**, N6, 403 (1994).
59. S.L. Dexheimer, M.D. Mittlemann, R.W. Schoenlien, W. Vareka, X.-D. Xiang, A. ZettL, C.V. Shank, in Ultrafast Phenomena VIII, Springer Series in Chem. Phys., **55**, 81 (1992).
60. S.D. Brorson, M.K. Kelly, U. Wenschuh, R. Buhleier, J. KuhL in Ultrafast Phenomena VIII, Springer Series in Chem. Phys. **55**, 354 (1992). S.D. Brorson, M.K. Kelly, U. Wenschuh, R. Buhleier, J. Kuhl, Phys. Rev. B**46**, 7329 (1992).
61. S.B. Fleischer, E.P. Ippen, G. Dresselhaus, M.S. Dresselhaus, A.O. Rao, P. Zhou, P.C. Eklund, Appl. Phys. Letters, **62**, 3241 (1993).
62. I.E. Kardash, V.S. Letokhov, Yu.E. Lozovik, Yu.A. Matveets, A.G. Stepanov, V.M. Farztdinov, Pis'ma ZhETF, **58**, 134 (1993). [JETP Letters, **58**, 138 (1993).]

63. V.M. Farztdinov, Yu.E. Lozovik, Yu.A. Matveets, A.G. Stepanov and V.S. Letokhov, J. Phys. Chem., **98**, 3290 (1994).
64. S.V. Chekalin, V.M. Farztdinov, E. Akesson, V. Sundstrem, Pis'ma ZhETF, **58**, 286 (1993). [JETP Letters, **58**, 295 (1993)].
65. J.L. Martins, N. Troullier, J.H. Weaver, Chem. Phys. Letters, **180**, 457 (1991); J.H. Weaver, J.L. Martins, T. Komeda, Y. Chen, T.R. Ohno, G.H. Kroll, N. Troullier, R.E. Haufler, R.E. Smalley, Phys. Rev. Letters, **66** 1741 (1991); J.H. Weaver, Acc. Chem. Res., **25**, 143 (1992).
66. R.W. Lof, M.A. van Veenendaal, B. Koopmans, A. Heessels, H.T. Jonkman and G.A. Sawatzky, Phys. Rev. Letters, **68**, 3926 (1992).
67. D.L. Lichtenberger, K.W. Nebesny, C.D. Ray, D.R Huffman and L.D. Lamb, Chem. Phys. Letters, **176**, 203 (1991).
68. P.L. Hansen, P.J. Fallon and W. Kratschmer, Chem. Phys. Letters, **181**, 367 (1991).
69. G. Gensterblum, J.J. Pireaux, P.A. Thiry, R. Caudano, J.P. Vigneron, Ph. Lambin, A.A. Lucas and W. Kratschmer, Phys. Rev. Letters, **67**, 2171 (1991).
70. E. Sohmen, J. Fink, and W. Kratschmer, Z. Phys. B **86**, 87 (1992); E. Sohmen, and J. Fink, Phys. Rev. B**47**, 14532 (1993).
71. I.V. Bezel S.V. Chekalin, Yu.A. Matveets, A.G. Stepanov, A.P. Yartsev and V.S. Letokhov, Chem. Phys. Letters, **218**, 475 (1994).
72. V.S. Letokhov, *Laser photoionization spectroscopy.* (Academic Press, Orlando), 1987, 353 pp.
73. V.M. Farztdinov, Yu.E. Lozovik and V.S. Letokhov, Chem. Phys. Lett, **218**, 475 (1994); Chem. Phys. Lett, **233**, 490 (1995).
74. H. Hohman, C. Callegari, S. Furrer, D. Grosenick, E.E.B. Campbell and I.V. Hertel. Phys. Rev. Lett. **73**(14), 1919 (1994).